Proceedings of the 28th IEEE
EMBS Annual International Conference
New York City, USA, Aug 30-Sept 3, 2006

Measurement of 2-D SpO_2 Distribution in Skin Tissue by Multispectral Imaging with Depth Selectivity Control

Hidenobu Arimoto

Abstract— **Two-dimensional hemoglobin oxygen saturation measurement is demonstrated by using the combination technique of multispectral imaging and the polarization control. Multispectral images are acquired at the wavelength range from 500 to 680 nm to observe the wavelength-dependent diffusely reflected light from the skin tissue. For eliminating the superficially reflected light from the skin, the skin tissue is illuminated by linearly polarized light and the polarization analyzer whose orientation is perpendicular to the illumination light is inserted in front of an imaging camera. The hemoglobin oxygen saturation levels corresponding to all image pixels are estimated by the partial least squares regression method with respect to each reflection spectrum. Mapping all the estimated values enables the oxygen saturation map across the observed tissue area.**

I. INTRODUCTION

Hemoglobin oxygen saturation (SpO_2) is defined as the percentage of bound oxygen to the total amount that can be bound. Generally, SpO_2 is measured by a pulse oximeter that utilizes differences of light absorptions at wavelengths from 650 to 900 nm because of the large difference in absorptions between oxyhemoglobin and deoxyhemoglobin and the presence of the isosbestic point around 800 nm [1]. Although the tissue and blood cause light scattering that results in the ambiguity of the light pass length, the blood pulsation enables the precise measurement of SpO_2 in the transmission arrangement of light sources and a detector. However, existing pulse oximeters measure SpO_2 values at only one point at a time, in addition, the clip-on type that is adopted by many compact pulse oximeters is not suitable for long-time monitoring. From these backgrounds, we have developed an imaging-based two-dimensional (2D) oxygen saturation measurement technique. The 2D oxygen saturation measurement has potential applications such as a long-time bedside monitoring for a neonate and a functional retinal imaging.

The developed 2D oxygen saturation measurement technique is based on the combination method of multispectral imaging and polarization control. Multispectral imaging is a technique for acquiring 2D images that retain the spectral information with respect to each pixel. In addition to providing structural properties, similar to ordinary imaging, multispectral imaging also provides spectral properties at all points across the measured area; therefore it is possible to obtain additional information such as the chemical characteristics of the object. The utilization of spectroscopy in application fields of biomedical functional measurements has long been attracted because of its non-invasive nature, and many useful applications have been reported such as non-invasive blood glucose measurement [2], cancer detection [3], and skin hydration measurement [4], [5]. Also, the application of multispectral imaging to biomedical measurement in fields such as endoscopy [6] and retinal imaging have been widely reported [7]. Although many pulse oximeters successfully measures SpO_2 by using only two wavelengths, we use more than 10 wavelength components because the imaging system observes diffusely reflected light from the skin tissue and variation of optical path lengths need to be compensated by a multivariate analysis.

The polarization control in the developed 2D oxygen saturation measurement is used for the depth-selective measurement in the skin tissue. Since the biological tissue scatters light, diffusely reflected light contains portions that propagates in various depths and path lengths. By utilizing the difference in the polarization states between incident light and detected light, superficially reflected light and deeply penetrated light can be separated [8], [9]. This technique is referred to as polarization imaging or polarization gating. When the blood oxygenation is measured by using light through the skin surface, the use of the polarization technique enables a reduction in the amount of diffuse reflected light from the avascular superficial layer of the skin. Sowa and co-workers have presented the PCA technique and the evaluation of the source-detector distance with avoiding specular reflection. [10], [11] The superiority of the polarization technique for eliminating specular reflection is characterized by fast processing of the depth selectivity in the 2D imaging technique before spectral analysis.

In this paper, we present the demonstration experiment of 2D blood oxygen saturation measurement that is based on multispectral imaging and polarization gating. The method of spectral analysis by using the multivariate regression technique is also explained in detail.

II. PRINCIPLES

This section provides the principles of spectroscopic approach for blood oxygenation levels and the polarization gating technique for the depth selective measurement. The spectral range between 400 and 600 nm is used for determining the SpO_2 levels in our technique; however, the change in this spectrum is smaller and the spectral profile of the hemoglobin absorption is finer than that for the longer wavelength range that is commonly used for pulse oximeters. The absorption coefficient of the hemoglobin with a high

H. Arimoto is with Photonics Research Institute, National Institute of Advanced Industrial Science and Technology, AIST East, Tsukuba, Japan arimoto-h@aist.go.jp

1-4244-0033-3/06/$20.00 ©2006 IEEE.

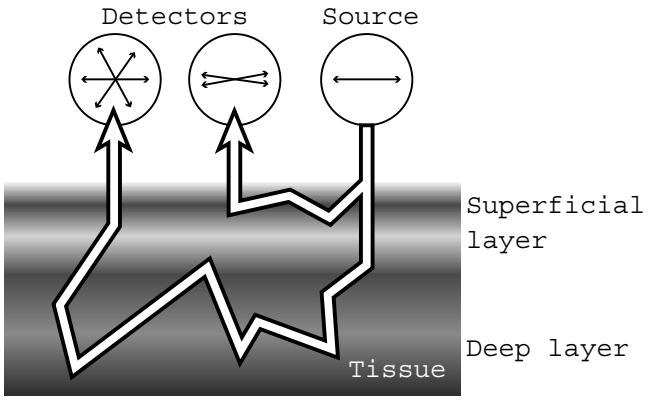

Fig. 1. Polarization states of incident and detected light depending on the propagation depths in the skin tissue. When linearly polarized light is incident on the skin surface, detected light, which is diffusely reflected from the superficial layer almost retains the original polarization state while detected light, which propagates in the deep layer is largely depolarized.

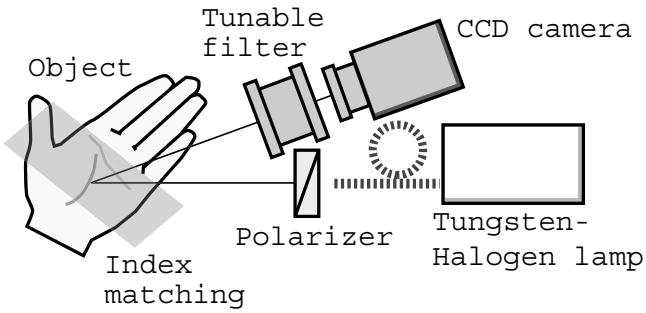

Fig. 2. Experimental setup for acquiring multispectral images with the polarization control. Linearly polarized light emitted from the light source and the linear polarizer illuminates the object. Reflected light passes through the liquid crystal tunable filter and is observed by a CCD camera. The polarization analyzer is included in the tunable filter.

SpO_2 level is larger than that of hemoglobin with a low SpO_2 level in the wavelength ranges shorter than 500 nm and between 530 and 545 nm and 570 and 584 nm. In our experiment, we use the spectral band ranging from 500 to 680 nm. The multispectral images are acquired by a wavelength tunable filter and an imaging camera. Since all the pixel points in the measured multispectral images have spectral information according to each pixel point, the spectral data is extracted from the measured data set. After extracting all spectra, the scattering effect is compensated by the multiplicative scattering correction (MSC) method, and then the compensated spectra were analyzed by the partial least squares (PLS) regression for developing the regression model and predicting the SpO_2 levels.

Next, we proceed to the principle of polarization gating. The polarization gating technique is introduced in this study in order to eliminate light from the superficial layer of the skin where capillaries, arteries and veins hardly exist. When incident light strikes the boundary of the skin surface, a portion of the light is reflected as specular reflection while an other portion propagates into the tissue. The light propagating in the tissue is scattered repeatedly depending on the scattering coefficients, which differ statistically at each layer such as the stratum corneum, epidermis, dermis, and subcutaneous layer. Hence, light propagating into a deep site of the skin is almost depolarized, while the superficial reflection retains the original scattering state as illustrated in Fig. 1. In order to achieve selective measurement based on these two polarization state, we use two polarizers that are placed behind the light source and in front of the imaging camera, respectively, as illustrated in Fig. 2. In order to eliminate the superficially reflected light, orientations of two polarizers are set to perpendicular that yields the depolarized light from a deeper site. It should be noted that the polarization gating technique does not provide discrete separation between the superficially reflected light and deeply penetrated light but these are cross-faded because the linearly polarized incident light becomes depolarized gradually as it propagates into the skin tissue. The depth properties that are provided by the polarization gating have been investigated with the Monte Carlo simulation method and reported by Liu and co-workers [12].

III. EXPERIMENT

Experiments were performed by using the same optical setup shown in Fig. 2. A monochromatic CCD camera (XC-EI50, sony, Tokyo, Japan) and a tip of an optical fiber bundle that is connected to a tungsten-halogen light source are arranged paraxially. The coaxial arrangement of the camera and the light source is an ideal setup for acquiring the images, however, we introduced a small angle between the source-object axis and the object-camera axis because of the limitations of the optical arrangement. Right in front of the CCD camera, a liquid crystal tunable filter (VariSpec VIS, Cambridge Research & Instrumentation, Inc., MA) is placed to scan the wavelength for acquiring the multispectral images. The tunable wavelength of the filter ranges from 400 to 720 nm with an FWHM of 20 nm, and the response time to switch the transmission wavelength is about 50 ms. For illuminating the object with linearly polarized light, a polarizer is placed behind the light source. The tunable filter includes its own polarizer inside the liquid crystal module; therefore, the source polarizer is oriented perpendicular directions with respect to the polarizer of the tunable filter. The CCD camera as well as the light source is placed at a distance of 20 cm from the object. The analog video signal from the CCD camera is transmitted to a frame grabber on a PC, and the image data is stored in an 8-bit digital format with a spatial resolution of 640x512.

In the demonstration experiment, the multispectral images of a palm were captured. Since the reflected intensity from the object was too weak, the spectral ranges from 400 to 500 nm and from 680 to 720 nm were excluded from the measurement. The multispectral images were acquired by scanning the wavelength ranging from 500 to 680 nm at intervals of 20 nm. Measurement time for acquiring 10 images was less than 1 s. All observed images were

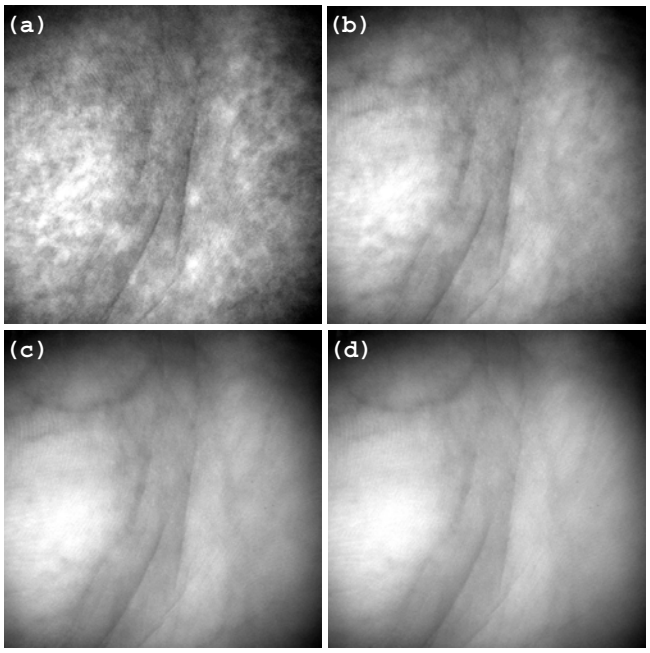

Fig. 3. Examples of the acquired images at wavelengths of (a) 580, (b) 600, (c) 620, and (d) 640 nm amongst 10 wavelength components. In images at the short wavelength range ((a) and (b)), capillary blood near the skin surface is seen while striated veins appear in images at the long wavelength range; (c) and (d).

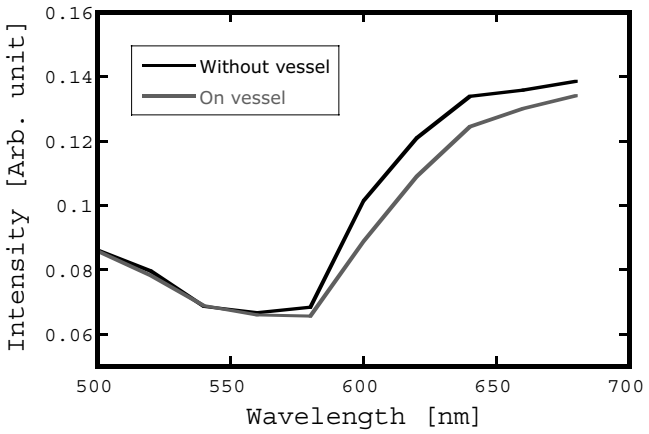

Fig. 4. Reflected intensity spectra observed at a point on a striated vein and a point without visible vessels. At the wavelength range from 500 to 580 nm, no significant differences are observed, however, the reflectance of the on-vessel point is smaller between 600 and 680 nm.

converted to the spectral reflectance by using the spectral sensitivity measured with a $BaSO_4$ plate. At the same time, the SpO_2 level on an index finger was monitored by a pulse oximeter (PULSOX-300, Konica Minolta, Tokyo, Japan). For comparing 2D oxygen saturation results between different SpO_2 levels, multispectral images at different SpO_2 levels were acquired by varying the breathing patterns. The maximum and the minimum SpO_2 levels monitored were 97% and 90%, respectively.

IV. RESULTS

Four examples of observed monochromatic images out of 10 acquired images (after compensation by the spectral sensitivity) are shown in Fig. 3. The measured size of original images is 640x512; however, only a 480x480 area at the center of each image is shown. The image of Fig. 3 (a) measured at the wavelength of 580 nm is covered with speckled spots. From the wavelength of 580 to 620 nm, the speckle spots become pale while striated vessels appear, and at 620 nm, the speckle spots almost disappear. The contrast of the striated vessels is maximum at 600 nm. For understanding these differences in images depending on the wavelength, it is necessary to consider the structure and the optical properties of skin layers and blood vessels. At the stratum corneum and the epidermis with the thickness of about a few hundreds micrometers, blood vessels hardly exist, while the capillary is located immediately under the basel laminae and the thick blood vessels are embedded in deeper sites. Generally, veins run in shallower sites than artery. Since the hemoglobin oxygenation in vein is considered to be lower than that of capillary, optical properties of blood in capillary and vein are also different. In the wavelength range from 500 to 580 nm, hemoglobin with any oxygenation levels exhibits strong absorption. Therefore the speckle spots seen over the images at the wavelengths of 580 and 600 nm are caused by absorption by the superficial capillary blood. Then a large amount of incident light is absorbed by the superficial capillary blood in the wavelength range shorter than 580 nm, and the deeper striated vessels do not appear in this range. For wavelengths longer than 600 nm, lesser absorption of the capillary blood results in deeper penetration of the incident light.

Next we investigate the spectra extracted from the multispectral images. Figure 4 shows the reflection spectra extracted from the multispectral images at a point on a striated vessel (denoted by "on vessel") and at a point where no vessel is seen (denoted by "without vessel"). As seen from the graphs, the two reflection spectra are almost the same in the wavelength range from 500 to 580 nm, and the on-vessel-spectrum is smaller in the range from 600 to 680 nm. Since the hemoglobin in the capillary blood releases oxygen, it has an intermediate SpO_2 level. This results in the without-vessel-spectrum. On the other hand, the on-vessel-spectrum resulted from the blood with low SpO_2 level. The absorption coefficient of the deoxygenated blood is considerably higher than that of oxygenated blood in the wavelength range from 600 to 800 nm; however, they do not exhibit a significant difference in the range of 500 to 580 nm. Therefore it seems reasonable to suppose that the visible striated vessels are veins with low SpO_2 blood. Further, it is also considered that generally, sites in which an artery travels are deeper than those in which vein travels and visible light can barely penetrate such deep sites. It should be mentioned that the oxyhemoglobin and deoxyhemoglobin exhibit different spectral properties at the wavelength around 550 nm, however, they were not observed in this experiment because of the lack of the spectral resolution of the wavelength tunable filter.

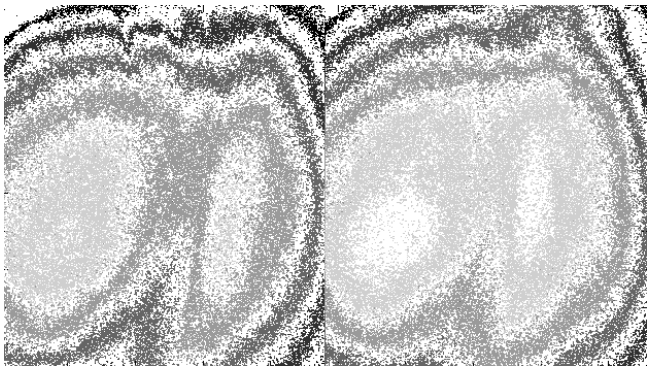

Fig. 5. Calculated SpO_2 level maps for the monitored SpO_2 values of (a) 92 and (b) 97% plotted with contours. Light dots represent high values. The image (b) consists of higher values than the image (a), which represents the relative oxygenation value of (b) is higher.

New 2D information can be calculated by multivariate processing with respect to all the spectrum extracted from each pixel. Focusing on the change in the spectrum depending on the SpO_2 level, we developed a PLS regression model with the SpO_2 level as responses and the spectra at each wavelength as the explanatory variables.

For developing the regression model to estimate the oxygen saturation levels, two different types of pixels were selected from the images captured in the experiment: one is a point on a visible striated vessel and the other is a point on an area without a visible vessel. This is because these two spectra can be considered to reflect the difference in the SpO_2 levels as seen from Fig.4. We selected 25 points from each of the two typical regions. Before developing the regression model, we adopted MSC to compensate for the signal variations. In general, MSC compensates two types of spectral variations: additive change (shift along the vertical axis) and multiplicative change (extension along the vertical axis). The type of the compensation to adopt is determined by repeating validations with evaluating errors. In this experiment, both the additive and multiplicative effects were corrected. The compensation parameters (shift and extension amounts) were determined by excluding the wavelengths from 580 to 680 nm because the change in the spectrum in this wavelength range is significantly affected by the oxygenation levels. Next, we set only two different response values for each pixel: 0 for pixels on the visible vessel and 1 for pixels without the vessel. This insufficiency in binding the response variables arises because we cannot determine the actual SpO_2 values corresponding to blood on each pixel. Therefore, a predicted result represents a relative change. In other words, the regression model was developed based on the similarity to the typical spectra whose signatures are significantly affected by SpO_2 values. The regression model was developed by using 50 calibration points (25 each on vessel and without vessel). The root-mean-square error obtained by the full-cross validation with four PLS factors was 0.20.

The regression model with four PLS factors were used after adopting additive and multiplicative MSC model. The result images are shown in Figs. 5 (a) and (b) as contour maps. The area shown in Fig. 5 is the same as that of Fig. 3. Each pixel value is the estimated response by using the PLS regression. Light dots represent the high value. It is evident that the predicted values in (b) are higher than those in (a) over the entire area. It should be noted that this method provides a relative comparison with respect to the SpO_2 levels. This implies that this technique can be useful in time-series measurements such as bedside monitoring of the same object. In other words, the absolute value measurement for SpO_2 with the wavelength range from 500 to 680 nm is not easy because an isolated isosbestic point between oxyhemoglobin and deoxyhemoglobin spectra is not present in this spectral range.

V. CONCLUSION

A new method for measuring 2D oxygen saturation level in the skin tissue was demonstrated based on multispectral imaging and polarization gating for the light penetration depth control. Reflected spectra were evaluated by the PLS regression for estimating the oxygen saturation levels according to all pixel points. The result of the oxygen saturation maps successfully exhibit the difference of two saturation levels.

REFERENCES

[1] W. Zijlstra, A. Buursma, and W. P. M. van der Roest, "Absorption spectra of human fetal and adult oxyhemoglobin, deoxyhemoglobin, carboxyhemoglobin, and methemoglobin," *Clin. Chem.*, vol. 37, pp. 1633–1638, 1991.

[2] M. A. Arnold, J. J. Burmeister, and G. W. Small, "Phantom glucose calibration models from simulated noninvasive human near-infrared spectra," *Anal. Chem.*, vol. 70, no. 9, pp. 1773–1781, 1998.

[3] A. S. Haka, K. E. Shafer-Peltier, M. Fitzmaurice, J. Crowe, R. R. Dasari, and M. S. Feld, "Diagnosing breast cancer by using raman spectroscopy," *Proc. Natl. Acad. Sci. USA*, vol. 102, no. 35, pp. 12 371–12 376, 2005.

[4] K. Martin, "In vivo measurements of water in skin by near-infrared reflectance," *Appl. Spectrosc.*, vol. 52, no. 7, pp. 1001–1007, 1998.

[5] H. Arimoto and M. Egawa, "Non-contact skin moisture measurement based on near-infrared spectroscopy," *Appl. Spectrosc.*, vol. 58, no. 12, pp. 1439–1446, 2004.

[6] E. Lindsley, E. S. Wachman, and D. L. Farkas, "The hyperspectral imaging endoscope: towards new in vivo cancer diagnostics," *Proc. SPIE*, vol. 5322, pp. 75–82, 2004.

[7] B. Khoobehi, J. M. Beach, and H. Kawano, "Hyperspectral imaging for measurement of oxygen saturation in the optic nerve head," *Invest. Ophthalmol.*, vol. 45, no. 5, pp. 1464–1472, 2004.

[8] R. R. Anderson, "Polarized light examination and photography of the skin," *Arch. Dermatol.*, vol. 127, pp. 1000–1005, 1991.

[9] J. M. Schmitt, A. H. Gandjbakhche, and R. F. Bonner, "Use of polarized light to discriminate short-path photons in a multiply scattering medium," *Appl. Opt.*, vol. 31, no. 30, pp. 6535–6546, 1992.

[10] M. G. Sowa, J. R. Payette, M. D. Hewko, and H. H. Mantsch, "Visible - near infrared multispectral imaging of the rat dorsal skin flap," *J. Biomed. Opt.*, vol. 4, pp. 474–481, 1999.

[11] M. G. Sowa, L. Leonardi, J. R. Payette, J. S. Fish, and H. H. Mantsch, "Near infrared spectroscopic assessment of hemodynamic changes in the earlypost-burn period," *Burns*, vol. 27, no. 3, pp. 241–249, 2001.

[12] Y. Liu, Y. Kim, X. Li, and V. Backman, "Investigation of depth selectivity of polarization gating for tissue characterization," *Opt. Express*, vol. 13, no. 2, pp. 601–611, 2005.